

## Supporting Information

1

2

### 3 Enhanced visible-light photodegradation of fluoroquinolone-based antibiotics 4 and *E. coli* growth inhibition using Ag-TiO<sub>2</sub> nanoparticles

5

6 Jiao Wang <sup>a</sup>, Ladislav Svoboda <sup>b,c</sup>, Zuzana Němečková <sup>d</sup>, Massimo Sgarzi <sup>a</sup>, Jiří Henych  
7 <sup>d</sup>, Nadia Licciardello <sup>a,‡\*</sup>, Gianaurelio Cuniberti <sup>a\*</sup>

8

9 <sup>a</sup> Institute for Materials Science and Max Bergmann Centre of Biomaterials, TU  
10 Dresden, 01062, Dresden, Germany

11 <sup>b</sup> IT4Innovations, VŠB – Technical University of Ostrava, 17. listopadu 15/2172, 708  
12 33 Ostrava, Czech Republic

13 <sup>c</sup> Nanotechnology Centre, CEET, VSB-Technical University of Ostrava, 17. listopadu  
14 15/2172, 708 33 Ostrava, Czech Republic

15 <sup>d</sup> Institute of Inorganic Chemistry, Czech Academy of Sciences, Husinec-Řež 1001, 250  
16 68 Řež, Czech Republic

17 <sup>‡</sup> Current address: International Iberian Nanotechnology Laboratory, Avenida Mestre  
18 José Veiga s/n, 4715-330 Braga, Portugal

19

20 \* Corresponding authors:

21 Nadia Licciardello, E-mail: nadia.licciardello@tu-dresden.de and

22 nadia.licciardello@inl.int;

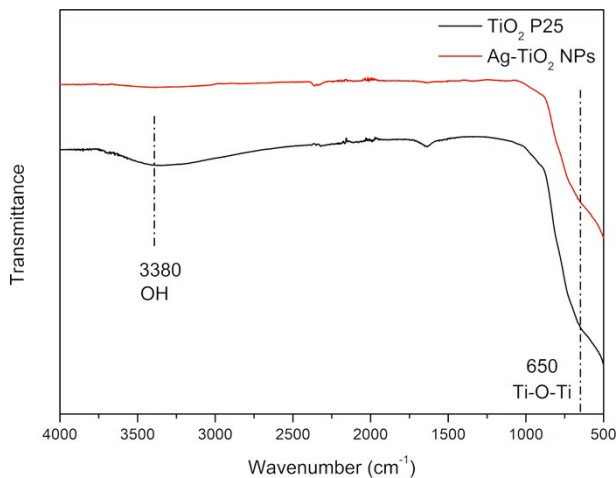
23 Gianaurelio Cuniberti, E-mail: gianaurelio.cuniberti@tu-dresden.de

24

25

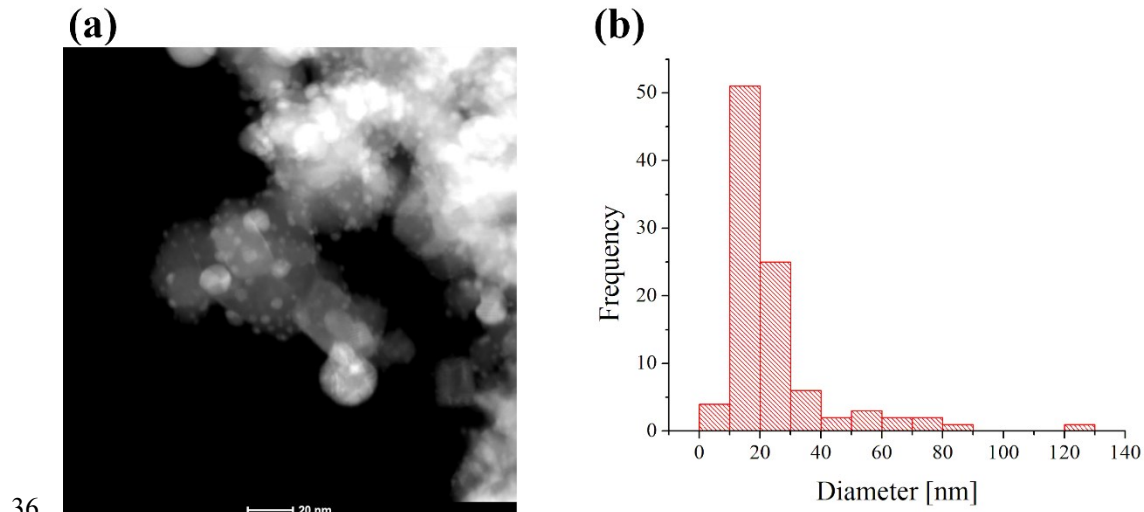
26 The ATR-FTIR spectra of TiO<sub>2</sub> P25 and Ag-TiO<sub>2</sub> NPs are shown in Figure S1. The  
27 band between 500 cm<sup>-1</sup> and 700 cm<sup>-1</sup> visible in both spectra of TiO<sub>2</sub> P25 and Ag-TiO<sub>2</sub>  
28 NPs corresponds to the Ti-O-Ti stretching vibrations<sup>1</sup>. The broad band at 3380 cm<sup>-1</sup>  
29 corresponds to the O-H stretching vibrations due to adsorption of water molecules from  
30 the moisture<sup>1</sup>. The FTIR spectrum of Ag-TiO<sub>2</sub> NPs resembles the one of TiO<sub>2</sub> NPs very  
31 much. However, the presence of Ag NPs in the Ag-TiO<sub>2</sub> NPs sample is hard to be

32 shown by FTIR spectroscopy since their concentration is low compared to the TiO<sub>2</sub>  
33 NPs.



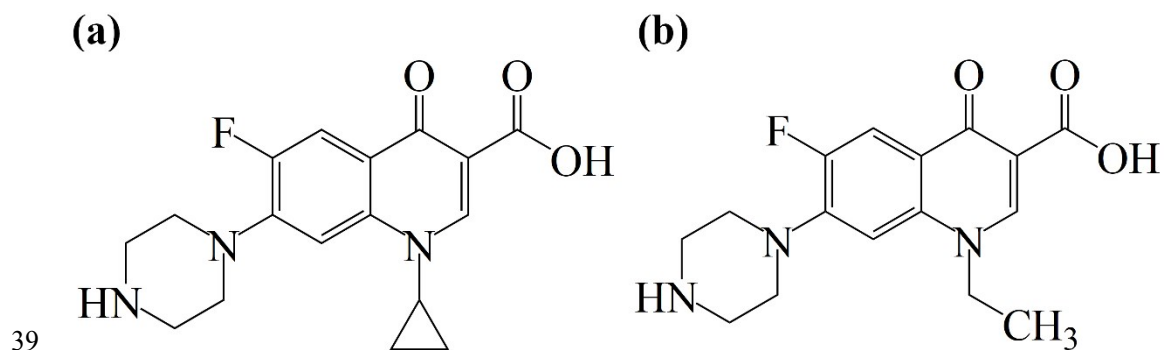
34

35 Figure S1. ATR-FTIR spectra of TiO<sub>2</sub> P25 and Ag-TiO<sub>2</sub> NPs



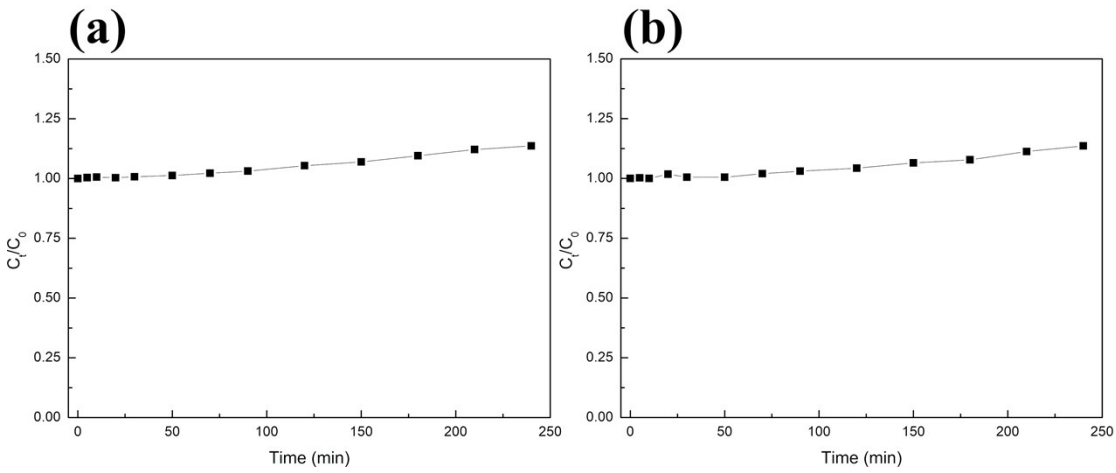
36

37 Figure S2. (a) STEM-HAADF micrograph of Ag/TiO<sub>2</sub> NPs; (b) Size distribution graph for Ag  
38 NPs obtained from Figure S2(a).



40 Figure S3. (a) Chemical structure of CIP; (b) Chemical structure of NFX.

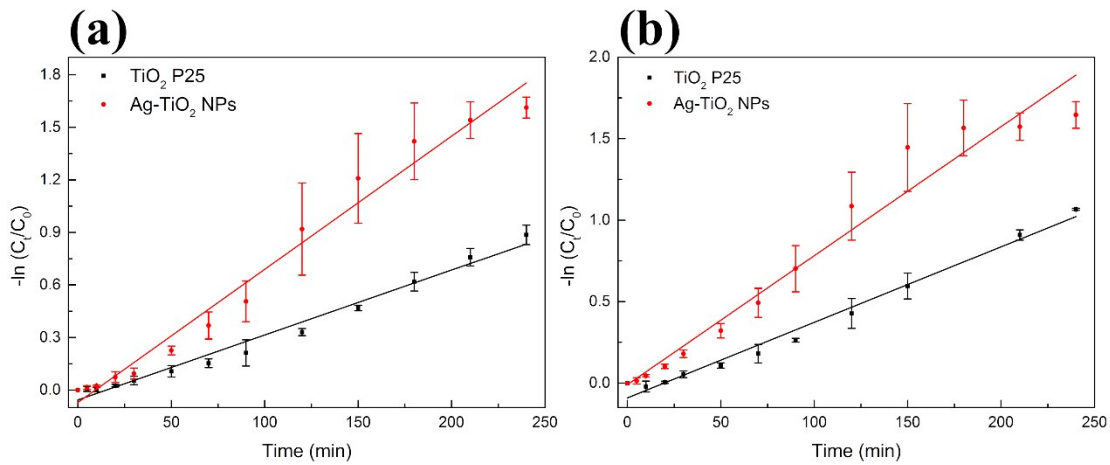
41



42

43

44 Figure S4. (a) Time-dependent variation of the concentration of CIP solution (3 mg/L, pH = 3)  
 45 upon exposure to visible light; (b) Time-dependent variation of the concentration of NFX  
 46 solution (3 mg/L, pH = 3) upon exposure to visible light.



47

48

49 Figure S5. Pseudo-first order kinetic fitting for: (a) the CIP solution (3 mg/L, pH = 3) upon  
 50 exposure to visible light in the presence of TiO<sub>2</sub> P25 (300 mg/L) and Ag-TiO<sub>2</sub> NPs (300 mg/L);  
 51 (b) the NFX solution (3 mg/L, pH = 3) upon exposure to visible light in the presence of TiO<sub>2</sub>  
 52 P25 (300 mg/L) and Ag-TiO<sub>2</sub> NPs (300 mg/L).

53

#### 54 References

55 1. E. H. Alsharaeh, T. Bora, A. Soliman, F. Ahmed, G. Bharath, M. G. Ghoniem, K. M.

56 Abu-Salah and J. Dutta, Sol-gel-assisted microwave-derived synthesis of anatase  
57 Ag/TiO<sub>2</sub>/GO Nanohybrids toward efficient visible light phenol degradation, *Catalysts*,  
58 2017, 7, 133.

59